analytical chemistry

Technical Note

Cite This: *Anal. Chem.* 2018, 90, 3703−3707

pubs.acs.org/ac

Portable Photoelectrochemical Device Integrated with Self-Powered Electrochromic Tablet for Visual Analysis

Qianhui Yang, Qing Hao, Jianping Lei,* and Huangxian Ju

State Key Laboratory of Analytical Chemistry for Life Science, School of Chemistry and Chemical Engineering, Nanjing University, Nanjing 210023, People's Republic of China

Supporting Information

ABSTRACT: A portable photoelectrochemical (PEC) device is developed by intergating a self-powered electrochromic tablet for visual analysis. The tablet consists of an electron-injector (EI) part for photo-to-electric conversion and an electrochromic (EC) part for visualized readout, which are coated with dye-sensitized titanium dioxide film and Ni-doped tungsten trioxide (WO_3) film, respectively. Under the illumination of a white LED light, the photoexcited electrons generated from EI part convey to EC part through the conductive inner side of indium tin oxide slide and would cause color change of the Ni-doped WO_3 film in the presence of protons. Furthermore, the Ni-doped WO_3 film exhibits excellent transmittance modulation of more than 80%, providing an enhanced signal for visual analysis. Using pyrophosphate ion (PPi) as a model analyte, we have successfully constructed a visualized PEC sensing platform based on the formation of blue-colored hydrogen tungsten bronzes via the hydrolysis reaction of PPi. Being equipped with a small light source and a dark box, the PEC tablet as a portable device can perform colorimetric measurement with good reversibility and stability. This smart PEC device provides important reference for future studies on the visual application in practice.

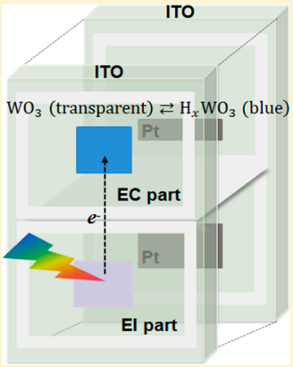

The photoelectrochemitry (PEC) is a promising low-cost and environment-friendly approach due to the efficient photo-to-electric conversion under light irradiation.[1−5] Generally, a conventional PEC instrument system includes a physical excitation source, a cell with a three-electrode system, and an electrochemical workstation for signal readout.[6−8] To miniaturize its size and develop PEC sensing system that meets the requirements of easy-to-use and portability, several efforts have been devoted to make great progresses. For instance, a series of PEC platforms, in which utilize chemiluminescence to replace the physical light source, have been developed to output an instantaneously amplified current for detection of protein, DNA, and other biomolecules.[9−12] It is still challenging to develop a low-cost, portable, fast, and easy-to-use PEC device to get rid of the expensive and sophisticated electrochemical workstation in practice.

Alternatively, colorimetric measurements based on different mechanisms such as conformation switch of dyes, enzymatic reaction of substrates, gold nanoparticle aggregation and electrochromism are extensively applied in visual detection with convenient signal readout.[13−17] In particular, electrochromic materials such as NiO, Co_2O_3, MoO_3, and WO_3, can reversibly change its color with certain optical modulation owing to double injection or extraction of electrons and ions,[18,19] and possess many desirable properties in signal transduction. Among these materials, tungsten trioxide (WO_3) demonstrates the distinctive advantages of fast switching speed, high coloration efficiency, and large transmittance modulation during the transformation between WO_3 and M_xWO_3[20,21] and thus makes WO_3 a favorable material for colorimetric analysis.[22−25] Meanwhile, metal ions such as Ni and Ti-doped WO_3 films have been proved superior to pure WO_3 films in optical modulation because of the increasement of crystal defects and surface roughness, resulting in an easier permeation of electrons and ions.[26,27] Therefore, the electrochromic material provides a favorable choice in finding a more convenient and instrument-free way for signal transduction in the PEC field.[28,29] Recently, a PEC sensing platform was constructed based on reducing prussian blue to prussian white through an external circuit for the detection of glycoprotein.[28] Different from the separation of PEC system, herein, an integrated PEC sensing device with miniaturized size is designed for the low-cost, fast, convenient, and visual detection.

The PEC sensing tablet composes of two parts: an electron-injector (EI) part coating dye-sensitized titanium dioxide film for photo-to-electric conversion and an electrochromic (EC) part on the basis of 2% Ni-doped tungsten trioxide (WO_3) film for visual detection (Figure 1). Furthermore, a portable PEC system was established by fixing the PEC tablet with a small homemade dark box containing the light source, meanwhile the light-leaking was completely prevented during sensing process (Figure S1). Under the illumination of a white LED light, the photoexcited electrons generated from EI part convey to the Ni-doped WO_3 film through the conductive inner side of indium tin oxide (ITO) glass and would cause the color change of EC part with the incorporation of proton into Ni-WO_3 film. The dependence of Ni-WO_3 electrochromism on proton

Received: December 15, 2017
Accepted: February 20, 2018
Published: February 20, 2018

DOI: 10.1021/acs.analchem.7b05232
Anal. Chem. 2018, 90, 3703−3707

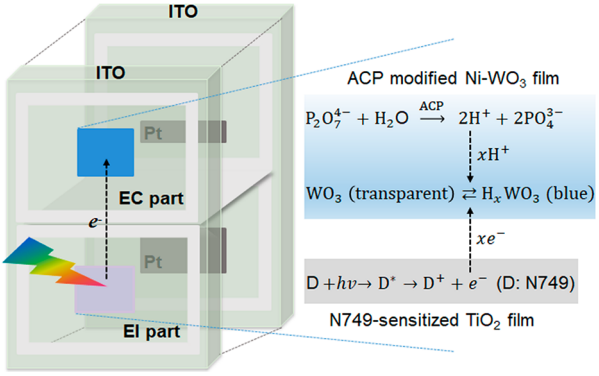

Figure 1. Schematic illustration of self-powered electrochromic tablet composing of electron-injector (EI) part and electrochromic (EC) part for visual analysis.

produces a novel PEC biosensing approach. Using pyrophosphate ions (PPi) as a model analyte,[30,31] a portable PEC device with good reversibility and stability was constructed for visual detection of PPi. This design greatly simplified the analytical apparatus and realized the proof of concept in visualized PEC detection.

EXPERIMENTAL SECTION

Materials and Reagents. Ammonium metatungstate hydrate $[(NH_4)_6H_2W_{12}O_{40}{\cdot}xH_2O]$ (AMH), anatase titanium dioxide (TiO_2), N749 black dye ($C_{69}H_{116}N_9O_6RuS_3$), acid phosphatase (ACP), sodium pyrophosphate, and Pluronic F127 were purchased from Sigma-Aldrich Inc. (St. Louis, MO, U.S.A.). Nitrate hexahydrate $[Ni(NO_3)_2{\cdot}6H_2O]$ was purchased from Sinpeuo Fine Chemical Co., Ltd. (Shanghai, China). ITO coated glass as the electrode material was purchased from Kaivo Electronic Components Co., Ltd. (Zhuhai, China), and was cut into 5.0 cm × 3.5 cm. All other chemicals were of analytical grade without further purification. All aqueous solutions were prepared using deionized water obtained from a Millipore water purification system (≥18 MΩ·cm, Milli-Q, Millipore).

Apparatus. Absorption spectra were recorded on an UV-3600 UV−vis-NIR spectrophotometer (Shimadzu Company, Japan). The morphology property of the films was studied using atomic force microscopy (AFM) system (Bruker Corp., Germany). The scanning electron microscopic (SEM) images were obtained on the ITO substrate by Hitachi S-4800 scanning electron microscope (Japan). Scanning electron microscopy-energy-dispersive X-ray spectroscopy (SEM-EDX) was used to analyze the elemental composition. The films were spin-coated on ITO glass using a KW-4A spin coater (SETCAS Electronics Co., Ltd.). Cyclic voltammetry (CV) and photovoltage measurements were performed on a CHI 630D electrochemical workstation (CH Instruments Inc., U.S.A.) with a three-electrode system consisting of a modified ITO as working electrode, a saturated calomel electrode as reference electrode and platinum wire as counter electrode.

Preparation of Ni-WO_3 Precursor Sol. Ni-WO_3 thin films on the ITO glass slides were prepared by sol−gel process. First, 1.0 g Pluronic F127 and 4.0 g AMH were dissolved in 8.0 mL of deionized water. Then the mixture was stirred at room temperature for 24 h to obtain a gel-like solution. Thereafter, 2% percentage of the Ni source ($Ni(NO_3)_2{\cdot}6H_2O$) was added to the solution with stirring. After dissolved, the solution was kept static for 6 h at 37 °C to obtain the precursor sol of Ni-WO_3.

Preparation of TiO_2 Paste. First, 2.0 g of commercial TiO_2 powder and 1.0 g PEG 20000 were dissolved in 18.0 mL of deionized water, then 2.5 mL of concentrated nitric acid were added to the solution. The mixture was stirred at room temperature overnight to obtain a well-distributed TiO_2 paste.

Preparation of Ni-WO_3 and TiO_2 Films. The Ni-WO_3 precursor solution was spin-coated onto the cleaned ITO substrate (5.0 cm × 3.5 cm) at 4000 rpm for 60 s. Before calcination, the edges of Ni-WO_3 on the ITO glass slide were trimmed to obtain a 0.7 cm × 1 cm size. Doctor blade method was used to prepare TiO_2 film on the same ITO glass slide. An adhesive tape (from 3 M Scotch) was used to control the size and thickness of TiO_2 film.[32] The whole film was then calcined at 400 °C for 1 h at a heating rate of 2 °C min^{-1} and cooled down to room temperature naturally. The ITO glass slide (only TiO_2 part) was then immersed in 0.3 mM ethanolic solution of N749 black dye for 2 h under dark condition to allow dye adsorption via bridging ester-like or bidentate interaction.[33] After washing with ethanol three times, the ITO slide was dried at 37 °C.

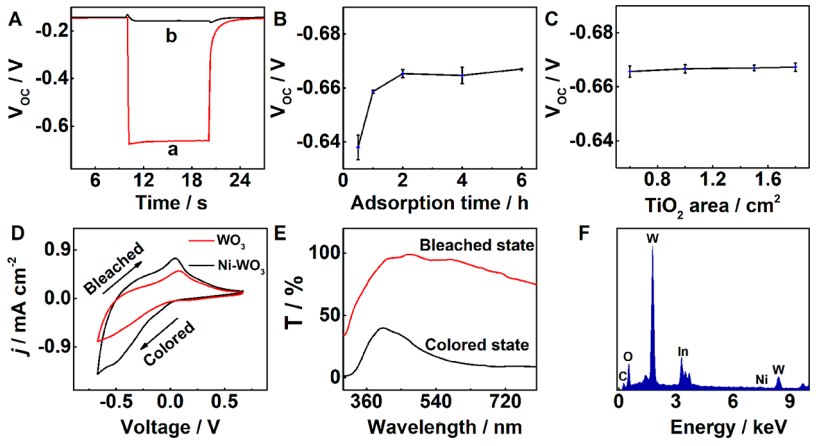

Figure 2. (A) Photovoltage curves of N749-sensitized (a) and bare (b) TiO_2 films on the ITO under white light (a LED flashlight, 2 W) irradiation. Effects of V_{OC} of N749-sensitized TiO_2 films on (B) dye adsorption times and (C) TiO_2 areas. (D) CV curves of WO_3 and Ni-WO_3 films on the ITO electrode at scan rate of 20 mV s^{-1} in 0.5 M H_2SO_4 electrolyte solution. (E) UV−vis transmittance spectra of Ni-WO_3 film at bleached state and colored state. (F) SEM-EDX mapping analysis of 2% Ni-doped WO_3 film.

DOI: 10.1021/acs.analchem.7b05232
Anal. Chem. 2018, 90, 3703−3707

Assembly of Smart PEC Device. To assemble the tablet, one Ni-WO_3/TiO_2 film modified ITO slide was sealed with another ITO slide, on which two thin platinum layers as counter electrodes were deposited using the sputtering technique in advance. Moreover, the tablet was divided into two chambers with rubber as EI part and EC part for providing the photovoltage and the colorimetric response, respectively. Prior to usage, an electrolyte liquid containing the I^-/I_3^- redox couple was injected into the EI part. Finally, the tablet was fixed in a dark box with the light source (a white LED light), and thus, a truly portable PEC device was constructed.

Performance for PPi Assay. Typically, 20 μL of 50 U L^{-1} ACP was modified on the Ni-WO_3 film in EC part by drop casting with a syringe. After about 30 min drying at 37 °C, the EC part of the as-prepared tablet was injected with PPi solution (1.0 mM acetate buffer, pH 5.0). After about 2 min irradiation of the EI part by a white LED light, the color response was distinguished by the naked eye, and then recorded by an ordinary digital camera. To use repeatedly, the EC part was washed with 0.1 M NaOH for three times.

The cycling stability of EC part was investigated by repeating the following steps: ACP was modified on Ni-WO_3 film first, then 1.8 mM PPi solution was added to the EC part of the tablet. After recording RGB_{avg}, the Ni-WO_3 film was washed with 0.1 M NaOH three times, and then discolored naturally within 3 h.

RESULTS AND DISCUSSION

Self-Powered Electron Source. Through the photo-to-electronic conversion, the N749-sensitized TiO_2 film provides a stable and constant photogenerated voltage for the colorimetric response of Ni-WO_3 film. As shown in Figure 2A, open-circuit voltages (V_{OC}) of bare (curve b) and sensitized (curve a) TiO_2 films under irradiation are about −0.15 and −0.67 V, respectively. In order to obtain better performance and stability, V_{OC} of electron source under different conditions were investigated. The effect of different adsorption times on V_{OC} are presented in Figure 2B, V_{OC} increased and reached a plateau at the dye adsorption time up to 2 h. In addition, as shown in Figure 2C, V_{OC} was furthermore found to be weakly dependent upon the area of TiO_2 film. Figure S2 displays the typical SEM image of the TiO_2 film with uniform-sized nanoparticles of about 20 nm. Meanwhile, the pores between the nanoparticles are evenly distributed to form a good mesoporous structure. These results demonstrate that the EI part could generate the sufficient and stable photovoltage for modulation of electrochromic process in EC part.

Preparation and Characterization of Ni-WO_3 Film. In order to improve the color modulation of Ni-WO_3 film, several parameters such as rotation rate, rotation time, and calcination temperature were evaluated by the univariate approach. The difference of color intensities (ΔRGB_{avg}) was monitored and normalized. As shown in Figure S3, ΔRGB_{avg} of Ni-WO_3 films reached a maximum value at the rotation rate of 4000 rpm min^{-1}, and then slightly declined with extension of rotation rate. Moreover, ΔRGB_{avg} increased remarkably along with the rotation time from 20 to 40 s, and reached a relatively stable value beyond 60 s (Figure S4). Therefore, we choose 4000 rpm min^{-1} and 60 s as the ideal rotation rate and time, respectively. Subsequently, with the calcination temperature increasing from 300 to 450 °C, ΔRGB_{avg} decreased slightly (Figure S5). Considering that Ni-WO_3 film would gradually change from amorphous to crystalline for producing better cycling stability as the temperature rises,[34] 400 °C was chosen as the favorable temperature to calcine Ni-WO_3 films.

CV measurements were tested to characterize the color change during scanning and evaluate ion storage capacities of Ni-WO_3 film. As shown in Figure 2D, a clear anodic peak around 0.05 V and a cathodic peak around −0.48 V can be observed for Ni-WO_3 (black line). As a result, a gradual color change of Ni-WO_3 film from transparent to blue can be clearly distinguished during the scanning from +0.67 to −0.67 V by the naked eye, which is attributed to the reduction of W^{6+} to W^{5+} when an electron is inserted into Ni-WO_3 film.[35,36] Meanwhile, the opposing color change was also observed during the scanning from −0.67 to +0.67 V. On the other hand, the areas enclosed by CV curves are closely related to the redox process of Ni-WO_3. Compared to undoped WO_3 (Figure 2D, red line), Ni-WO_3 film (Figure 2D, black line) showed an enhanced anodic and cathodic current density. The charge densities of the Ni-WO_3 films in the insertion and extraction electron process are calculated to be 20.46 and 22.51 mC cm^{-2}, respectively. Therefore, Ni-WO_3 composite film possesses a great higher ion storage capacity than the undoped WO_3.

The optical modulation property of Ni-WO_3 film was investigated after CV test for five cycles. Figure 2E shows the transmittance of the Ni-WO_3 film in bleached (red line) and colored (black line) states corresponding to transparent and a deep blue color, respectively, in the wavelengths ranging from 300 to 800 nm. Ni-WO_3 film exhibits excellent optical modulation in visible light range, accompanied by an average optical modulation ($\Delta T = T_b - T_c$, where T_b and T_c represent the enhanced transmittance in the bleached and colored state, respectively) of about 80% for transmittance at 600 nm.

The typical SEM image in Figure S6 and AFM image in Figure S7A exhibit the porous microstructure of as-prepared Ni-WO_3 film. Compared with the WO_3 film (Figure S7B), the surface of Ni-WO_3 film became rougher and more vertically arranged, which provides more active sites, suggesting that Ni doping leads to a significant microstructure change of WO_3 film. Meanwhile, the increased holes in the surface of Ni-WO_3 films contribute to smooth migration of protons and therefore lead to a better coloration ability.

Further, the elemental composition of Ni-WO_3 film was confirmed with SEM-EDX mapping analysis. As shown in Figure 2F, the EDX data clearly ascertains the coexistence of Ni and W elements in the film. The specific distribution of three elements including W, O and Ni can be seen in Figure S8, indicating the homogeneous doping of Ni in WO_3 film.

Electrochromic Assay for PPi. PPi plays significant roles in several biochemical and chemical processes. It has been reported that PPi could be used as a potential biomarker to monitor or diagnose a number of diseases, in terms of their levels.[37] Thus, the tablet was employed to construct a visualized PEC sensor for PPi. Along with the hydrolysis of PPi into orthophosphate by ACP modified on Ni-WO_3 film in EC part, the released protons were readily injected into the Ni-WO_3 film. At the same time, photoelectrons generated from EI part under a white LED light irradiation conveyed to EC part through the conductive inner side of ITO and injected into Ni-WO_3 film, resulted in the formation of hydrogen tungsten bronzes (H_xWO_3) and bringing Ni-WO_3 film to different color states. The electrochromic process can be described as shown in Figure 1, according to the previous report.[38]

The color of Ni-WO_3 film on ITO glass changes gradually from transparent to blue as the concentration of PPi increases.

DOI: 10.1021/acs.analchem.7b05232
Anal. Chem. 2018, 90, 3703−3707

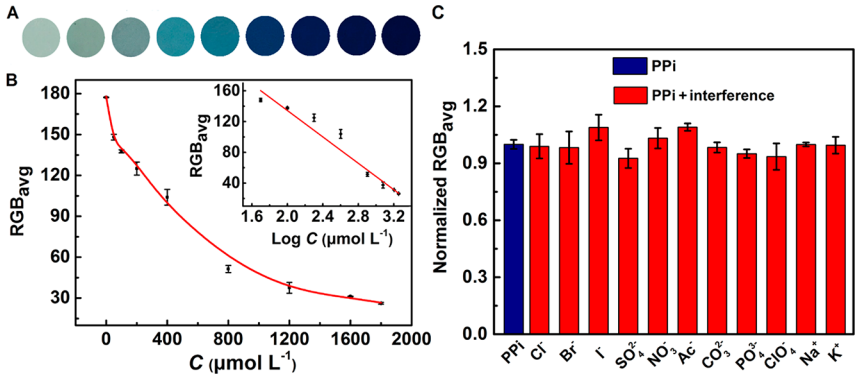

Figure 3. (A) Photographic images of ACP modified Ni-WO_3 film of EC part in the presence of 0, 50, 100, 200, 400, 800, 1200, 1600, and 1800 μM PPi after 2 min irradiation of EI part by LED light. (B) Plot of mean color intensity (RGB_{avg}) vs PPi concentration. Inset: linear relationship between RGB_{avg} vs logarithm value of PPi concentration. (C) Selectivity of as-established PEC device toward PPi in the presence of various interferences (5.0 equiv).

The variation of color and transmittance of the Ni-WO_3 film can be seen from images shown in Figure 3A. The color change can be clearly distinguished by the naked eye when the concentration of PPi reached 100 μM. In addition, the inset in Figure 3B showed a linear relationship between RGB_{avg} value obtained from Adobe Photoshop software and logarithm value of PPi concentration, with a linear regression correlation coefficient of 0.993 in a range of 50 μM to 1.8 mM. The detection limit calculated by 3σ rule, was estimated to be 31.1 μM, which is comparable to previously reported fluorescence assay.[39] Based on the potable PEC device, the determination of PPi was realized by both naked eyes and reading color intensities from Adobe Photoshop.

Selectivity of Portable PEC Device. The selectivity assessment to PPi was evaluated by mixing 5.0 equiv of several interfering substances with 1.0 equiv of PPi. The color responses were monitored by RGB_{avg}. From Figure 3C, the coexistence of interferences such as Cl^-, Br^-, I^-, SO_4^{2-}, NO_3^-, Ac^-, CO_3^{2-}, PO_4^{3-}, and ClO_4^- showed little influence on the colorimetric response of PPi while the cations such as K^+ and Na^+ are too big to be injected into the as-prepared Ni-WO_3 films. Therefore, these results demonstrate a high selectivity of the proposed platform toward PPi.

Stability of Portable PEC Device. For further applications, long-term durability is also an important requirement for the portable PEC tablet. As shown in Figure 4A, the EC part could be repeated for more than 50 times, while ΔRGB_{avg} was only slightly decreased during the cycling. Moreover, the EI part remained highly stable during 50 times cycling (Figure 4B). The relative standard deviations of five measurements of RGB_{avg} in the bleached and colored state were calculated to be 0.2% and 2.3%, while 1.6% and 0.2% for V_{OC} before and after irradiation. These results demonstrate the good cycling stability and repeatability of the as-established PEC device.

CONCLUSIONS

In summary, a portable PEC device was successfully established by integrating self-powered electrochromic tablet with a LED light for visual analysis. In the smart system, the photoexcited charges generated from EI part provides the sufficient and stable photovoltage, and modulates electrochromic process in EC part through electron transfer across the conductive inner side of ITO slide. Thus, this method avoided the external electrochemical workstation for signal readout. Moreover, the Ni-doped WO_3 film synthesized through a simple sol−gel spin coating technique exhibited excellent optical modulation of about 80%. The feasibility of the constructed tablet was confirmed experimentally with good selectivity and favorable stability by the determination of PPi. The integrated PEC device greatly simplified the analytical apparatus and provides a promising application in visualized PEC detection.

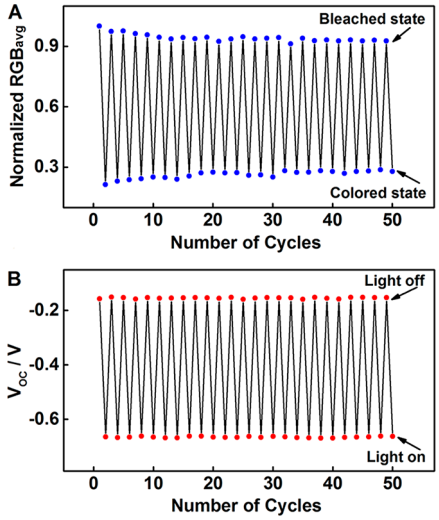

Figure 4. Cycling stability of (A) Ni-WO_3 film evaluated through RGB_{avg} at bleached and colored states, and (B) N749-sensitized TiO_2 electrode evaluated through photovoltages with and without irradiation.

ASSOCIATED CONTENT

Supporting Information

The Supporting Information is available free of charge on the ACS Publications website at DOI: 10.1021/acs.analchem.7b05232.

Supplementary figures showing photograph of portable PEC device, SEM image of TiO_2 film, optimization conditions in Ni-WO_3 film preparation, SEM image of Ni-WO_3 film, AFM images of Ni-WO_3 and WO_3 film, and element mapping of Ni-WO_3 film (PDF).

AUTHOR INFORMATION

Corresponding Author

*Phone/Fax: +86-25-89681922. E-mail: jpl@nju.edu.cn.

DOI: 10.1021/acs.analchem.7b05232
Anal. Chem. 2018, 90, 3703−3707

ORCID

Jianping Lei: 0000-0002-3594-180X
Huangxian Ju: 0000-0002-6741-5302

Notes

The authors declare no competing financial interest.

■ ACKNOWLEDGMENTS

This research was supported by the National Key Technologies R&D Program (2016YFC0302500), and National Natural Science Foundation of China (21375060, 21635005, 21675084).

■ REFERENCES

(1) Cowan, A. J.; Durrant, J. R. *Chem. Soc. Rev.* **2013**, *42*, 2281−2293.
(2) Hao, N.; Zhang, Y.; Zhong, H.; Zhou, Z.; Hua, R.; Qian, J.; Liu, Q.; Li, H. N.; Wang, K. *Anal. Chem.* **2017**, *89*, 10133−10136.
(3) Trashin, S.; Rahemi, V.; Ramji, K.; Neven, L.; Gorun, S. M.; De Wael, K. *Nat. Commun.* **2017**, *8*, 16108.
(4) Yan, Z. Y.; Wang, Z. H.; Miao, Z.; Liu, Y. *Anal. Chem.* **2016**, *88*, 922−929.
(5) Devadoss, A.; Sudhagar, P.; Terashima, C.; Nakata, K.; Fujishima, A. *J. Photochem. Photobiol., C* **2015**, *24*, 43−63.
(6) Hao, Q.; Shan, X. N.; Lei, J. P.; Zang, Y.; Yang, Q. H.; Ju, H. X. *Chem. Sci.* **2016**, *7*, 774−780.
(7) Riedel, M.; Hölzel, S.; Hille, P.; Schörmann, J.; Eickhoff, M.; Lisdat, F. *Biosens. Bioelectron.* **2017**, *94*, 298−304.
(8) Zhao, W. W.; Xu, J. J.; Chen, H. Y. *Biosens. Bioelectron.* **2017**, *92*, 294−304.
(9) Wang, Y. H.; Ge, L.; Wang, P. P.; Yan, M.; Ge, S. G.; Li, N. Q.; Yu, J. H.; Huang, J. D. *Lab Chip* **2013**, *13*, 3945−3955.
(10) Zhang, X. R.; Zhao, Y. Q.; Zhou, H. R.; Qu, B. *Biosens. Bioelectron.* **2011**, *26*, 2737−2741.
(11) Zhang, Y.; Sun, G. Q.; Yang, H. M.; Yu, J. H.; Yan, M.; Song, X. R. *Biosens. Bioelectron.* **2016**, *79*, 55−62.
(12) Tu, W. W.; Wang, W. J.; Lei, J. P.; Deng, S. Y.; Ju, H. X. *Chem. Commun.* **2012**, *48*, 6535−6537.
(13) Valderrey, V.; Bonasera, A.; Fredrich, S.; Hecht, S. *Angew. Chem., Int. Ed.* **2017**, *56*, 1914−1918.
(14) Welter, M.; Verga, D.; Marx, A. *Angew. Chem., Int. Ed.* **2016**, *55*, 10131−10135.
(15) Wang, P.; Lei, J. P.; Su, M. Q.; Liu, Y. T.; Hao, Q.; Ju, H. X. *Anal. Chem.* **2013**, *85*, 8735−8740.
(16) Zloczewska, A.; Celebanska, A.; Szot, K.; Tomaszewska, D.; Opallo, M.; Jönsson-Niedziolka, M. *Biosens. Bioelectron.* **2014**, *54*, 455−461.
(17) Soh, J. H.; Lin, Y. Y.; Rana, S.; Ying, J. Y.; Stevens, M. M. *Anal. Chem.* **2015**, *87*, 7644−7652.
(18) Cai, G. F.; Darmawan, P.; Cui, M. Q.; Chen, J. W.; Wang, X.; Eh, A. L.; Magdassi, S.; Lee, P. S. *Nanoscale* **2016**, *8*, 348−357.
(19) Zhao, Q. W.; Li, Z.; Deng, Q.; Zhu, L. C.; Luo, S. L.; Li, H. *Electrochim. Acta* **2016**, *210*, 38−44.
(20) Zhou, X. F.; Zheng, X. L.; Yan, B.; Xu, T.; Xu, Q. *Appl. Surf. Sci.* **2017**, *400*, 57−63.
(21) Koo, B. R.; Ahn, H. J. *Nanoscale* **2017**, *9*, 17788−17793.
(22) Marques, A. C.; Santos, L.; Costa, M. N.; Dantas, J. M.; Duarte, P.; Goncalves, A.; Martins, R.; Salgueiro, C. A.; Fortunato, E. *Sci. Rep.* **2015**, *5*, 9910.
(23) Tanaka, S.; Adachi, K.; Yamazaki, S. *Analyst* **2013**, *138*, 2536−2539.
(24) Kalagi, S. S.; Mali, S. S.; Dalavi, D. S.; Inamdar, A. I.; Im, H.; Patil, P. S. *Synth. Met.* **2011**, *161*, 1105−1112.
(25) Lee, Y. A.; Kalanur, S. S.; Shim, G.; Park, J.; Seo, H. *Sens. Actuators, B* **2017**, *238*, 111−119.
(26) Karuppasamy, A. *Appl. Surf. Sci.* **2015**, *359*, 841−846.
(27) Zhou, J. L.; Wei, Y. X.; Luo, G.; Zheng, J. M.; Xu, C. Y. *J. Mater. Chem. C* **2016**, *4*, 1613−1622.
(28) Gao, C. M.; Wang, Y. H.; Yuan, S.; Xue, J.; Cao, B. Q.; Yu, J. H. *Biosens. Bioelectron.* **2017**, *90*, 336−342.
(29) Li, L.; Zhang, Y.; Zhang, L. N.; Ge, S. G.; Liu, H. Y.; Ren, N.; Yan, M.; Yu, J. H. *Anal. Chem.* **2016**, *88*, 5369−5377.
(30) Qian, Z. S.; Chai, L. J.; Zhou, Q.; Huang, Y. Y.; Tang, C.; Chen, J. R.; Feng, H. *Anal. Chem.* **2015**, *87*, 7332−7339.
(31) Sun, J.; Yang, F.; Yang, X. R. *Nanoscale* **2015**, *7*, 16372−16380.
(32) Coronado, E.; Galán-Mascarós, J. R.; Martí-Gastaldo, C.; Palomares, E.; Durrant, J. R.; Vilar, R.; Gratzel, M.; Nazeeruddin, M. K. *J. Am. Chem. Soc.* **2005**, *127*, 12351−12356.
(33) Rochford, J.; Chu, D.; Hagfeldt, A.; Galoppini, E. *J. Am. Chem. Soc.* **2007**, *129*, 4655−4665.
(34) Caruso, T.; Castriota, M.; Policicchio, A.; Fasanella, A.; De Santo, M. P.; Ciuchi, F.; Desiderio, G.; La Rosa, S.; Rudolf, P.; Agostino, R. G.; Cazzanelli, E. *Appl. Surf. Sci.* **2014**, *297*, 195−204.
(35) Bange, K. *Sol. Energy Mater. Sol. Cells* **1999**, *58*, 1−131.
(36) Reyes-Gil, K. R.; Stephens, Z. D.; Stavila, V.; Robinson, D. B. *ACS Appl. Mater. Interfaces* **2015**, *7*, 2202−2213.
(37) Ma, J. L.; Yin, B. C.; Wu, X.; Ye, B. C. *Anal. Chem.* **2016**, *88*, 9219−9225.
(38) Li, Y. Q.; Chen, D. H.; Caruso, R. A. *J. Mater. Chem. C* **2016**, *4*, 10500−10508.
(39) Lohani, C. R.; Kim, J. M.; Chung, S. Y.; Yoon, J.; Lee, K. H. *Analyst* **2010**, *135*, 2079−2084.

DOI: 10.1021/acs.analchem.7b05232
Anal. Chem. 2018, 90, 3703−3707